*Kovove Mater. 58 2020 363–369*
*DOI: 10.4149/km_2020_5_363*



# Microstructure and fracture mechanism of Cu-$Y_2O_3$ composite

O. Velgosova[1]*, S. Nagy[2], M. Besterci[3], V. Puchy[3]

[1]*Institute of Materials and Quality Engineering, Faculty of Materials, Metallurgy and Recycling, Technical University of Košice, Letná 9/A, 042 00 Košice, Slovak Republic*
[2]*Institute of Materials and Machine Mechanics, Slovak Academy of Sciences, Dúbravská cesta 9/6319, 845 13 Bratislava, Slovak Republic*
[3]*Institute of Materials Research, Slovak Academy of Sciences, Watsonova 47, 040 01 Košice, Slovak Republic*

Received 26 June 2020, received in revised form 7 July 2020, accepted 9 July 2020

**Abstract**

This work aimed to examine the structure of Cu-$Y_2O_3$ composite, analyse the fracture mechanism, and propose the model of fracture. The in-situ tensile test in SEM was used for direct observation of the process of deformation and fracture. Microscopic analysis revealed that Cu matrix grains are spherical with a mean diameter of ∼ 500 nm. EDX and selected area electron diffraction confirmed the presence of $Y_2O_3$ particles. Particles can be divided, according to the size, into two categories: smaller A (up to 20 nm) and more significant B (20–100 nm). The in-situ tensile test in SEM showed that the first cracks were created on the particle-matrix interfaces and in the triple point. Subsequent coalescence was observed, and we assumed that the cracks propagate along the grain boundaries. The fracture surface has a transcrystalline ductile character. Based on the in-situ observations and analysis, we proposed the model of fracture mechanism.

K e y w o r d s: Cu composite, $Y_2O_3$, high-resolution scanning transmission electron microscopy (HRSTEM), structure, fracture mechanism

## 1. Introduction

Recently, materials with specific properties have attracted a lot of attention. Today, advanced materials that are characterised not only by unique properties such as high strength, excellent conductivity, superior softening resistance, thermal or chemical resistance but also by a combination of these properties are required. The researchers try to achieve the desired unique properties by a combination of different matrices (Cu, Al, Mg, ...) and secondary phases ($Al_2O_3$, TiO, $Y_2O_3$, SiC, $ThO_2$, CNT, fullerenes, ...) [1–5]. Composites with unique properties can be prepared by various techniques; the bases include casting and powder metallurgy [6–9]. Carro et al. [10] fabricated Cu-$Y_2O_3$ dispersion strengthened composite by two different routes: casting and powder metallurgy (cryomilling and mechanical alloying). They found that the powder metallurgy route compared with the casting presents a significant dispersion of oxide nanoparticles inside the copper grains, the smallest grain size, and the highest microhardness. The potential of rapid solidification in $Y_2O_3$ dispersion strengthened copper alloy was analysed in work [11]. Authors confirmed that the spatial distribution of the oxide obtained in the internally oxidised powders was far from optimal for dispersion strengthening, even though the individual oxide particles are in the desired size range [11]. It is clear, that in some cases, powder metallurgy is more advantageous because this method makes it possible to combine materials that cannot be prepared by conventional melting methods. Using appropriate conditions of powders treatment it is possible to obtain a good dispersion of secondary phase in the matrix.

Copper is one of the essential materials in terms of high electrical and thermal conductivity. But pure copper is not suitable for use at higher temperatures, mainly due to its low strength. A lot of works have been focused on finding a suitable combination of copper matrix and reinforcing phase to achieve proper strength at elevated temperatures [11–13]. Copper-

*Corresponding author: tel.: +421 55 602 2533; fax: +421 55 602 2770; e-mail address: oksana.velgosova@tuke.sk

-based materials, in combination with the appropriate secondary phase, can also provide an optimal combination of good electrical conductivity and superior softening resistance [14–17]. Notably, a combination of Cu and $Y_2O_3$, $Al_2O_3$, or other rear metals is suitable for their excellent thermodynamic stability. Yttrium oxide is one of the promising materials for improving the properties of the Cu matrix. It is often used as a single secondary phase or in combination with other oxides as $Al_2O_3$, TiB + $Y_2O_3$, $La_2O_3$, $Al_2O_3$ + $Y_2O_3$ + CaO, $Y_2O_3$ + $ZrO_2$, TiB + TiC + $Y_2O_3$ [2, 3, 5, 7, 19, 20].

The chemical, physical and mechanical properties of dispersion strengthened composites and the methods of their improvement are well known. At the same time, a little attention has been paid on the mechanism of fracture. The study of cracks initiation and analysis of the processes/ways of their propagation can help better understand the interfacial interactions, the influence of the morphology of the matrix grains and particles on fracture mechanism of composite materials prepared by powder metallurgy route. The method of the "in-situ" tensile test in SEM is the best method for investigations of fracture mechanisms because it enables us to observe and document deformation processes directly. Thank to which, the initiation and development of the plastic deformation, initiation of cracks, and final fracture can be observed in real-time and reliably described.

This work aimed to characterise the structures of Cu-$Y_2O_3$ composite and also to analyse the distribution, shape and size of $Y_2O_3$-phase. Based on the "in-situ" observation of fracture mechanism of Cu-$Y_2O_3$ composite system, also try to propose the damage model concerning the presented phase.

## 2. Materials and methods

The method of mechanical alloying was used for preparing of Cu-$Y_2O_3$ composite material. The copper powder and 2 wt.% (3.54 vol.%) of $Y_2O_3$ powder, with the grain size of ~ 75 μm and 20–50 μm, respectively, were milled in an attritor under a protective atmosphere of argon (99.96 %) at 600 rpm for 16 h. The received mixture of powders was subsequently compacted by cold pressing, hot extrusion at 750–800 ℃, and sintering.

For the investigation, very small flat tensile test pieces, with 0.15 mm thickness were prepared by electro erosive machining, keeping the loading direction identical to the direction of extrusion, Fig. 1.

The specimens were ground and polished down to a thickness of approximately 0.1 mm. Finally, the specimens were polished by ion beam milling with PIPS instrument. The test pieces were fitted into the special deformation grips in the electron microscope Jeol SEM 5310, which enabled direct observation of the deformation. Based on direct observation of both the deformation and failure processes of the test pieces, it was possible to detect the crack initiation and propagation. Quantitative and qualitative analyses of secondary phases and matrix were realised using metallography, scanning electron microscopy (SEM), energy-dispersive X-ray spectroscopy (EDX), transmission electron microscopy (TEM), electron diffrac-

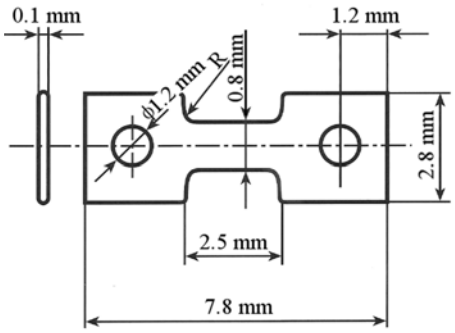


Fig. 1. Tensile test specimen.

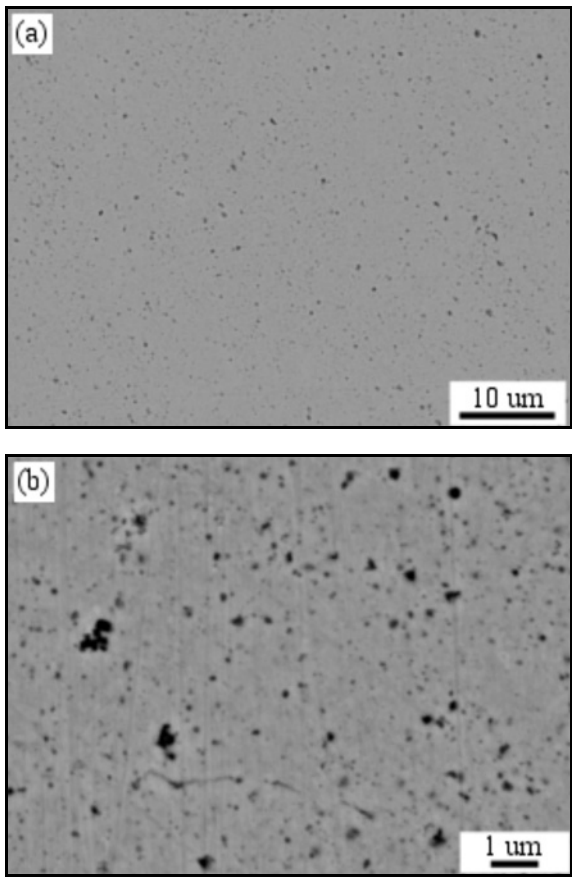


Fig. 2. The microstructure of the composite (a) with a detail of the homogeneous $Y_2O_3$ particles distribution (b).

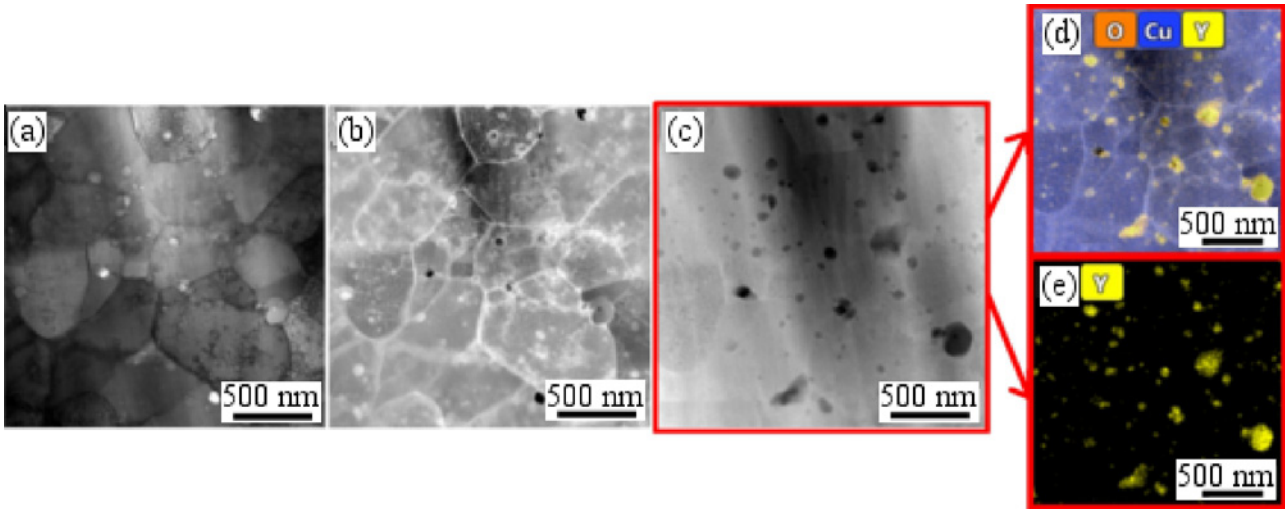


Fig. 3. HRSTEM microstructure of the composite at different detectors: bright field – BF (a), dark field – DF (b), HAADF image of the microstructure which represents the $Y_2O_3$ particles (c), EDS map of O, Cu, Y HAADF (d), and EDS map of yttrium (e).

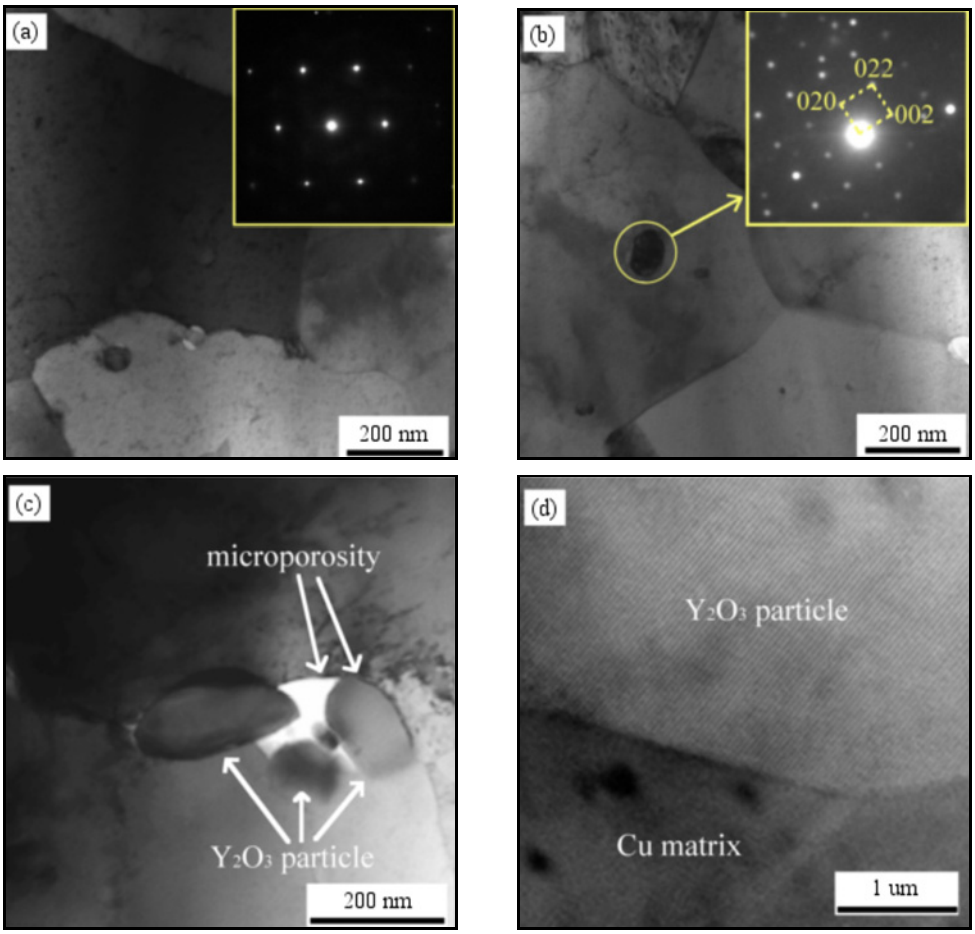


Fig. 4. TEM and HRSTEM microstructure reveal the Cu matrix with SAED pattern (a), $Y_2O_3$ particle with SAED pattern, particle clustering with micro-porosity (c), and particle-matrix interface (d).

tion and high-resolution scanning transmission electron microscopy (HRSTEM), and selected area electron diffraction (SAED).

## 3. Results and discussion

The microstructure of prepared composite mate-

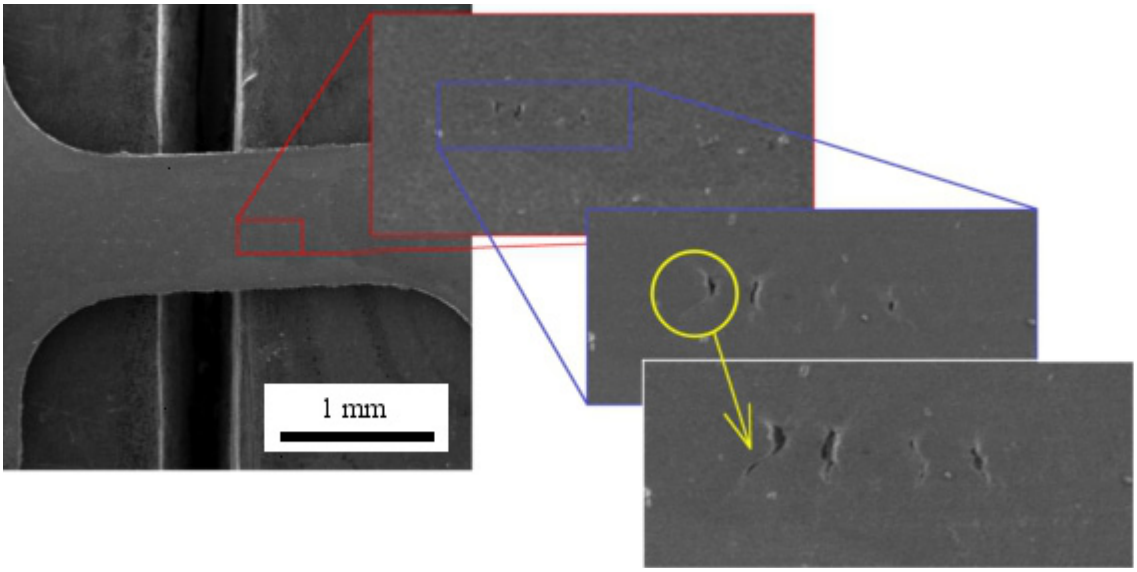


Fig. 5. SEM images of crack initiation and propagation behaviour.

rial can be seen in Fig. 2. COMPO mode material contrast in the scanning electron microscopy shows a homogeneous distribution of secondary $Y_2O_3$-phase in Cu matrix. However, at higher magnification particle clustering is evident also.

The detailed sight on matrix grains and $Y_2O_3$ particles shape, size, and distribution in the matrix is in Fig. 3. HRSTEM with EDS mapping was used to identify the micro- and nanoparticles of $Y_2O_3$ in the Cu matrix. The spherical Cu matrix grain size with a mean diameter of $\sim 500$ nm is also evident from the dark field image Fig. 3b. The HAADF detector shows the material contrast, which results in a better view of the $Y_2O_3$ particles. The particle distribution is also evident from the EDX map, showing the Y element, Fig. 3c. HRSTEM observation revealed the presence of spherical particles located inside the Cu grains as well as on grain boundaries. It is also evident that the two categories of particles are presented: category A – small particles up to 20 nm, and category B – larger particles from 20–100 nm.

Crystallographic identification was examined with TEM. SAED pattern reveals us the Cu matrix with cubic lattice in the zone axis of [1 0 1], Fig. 4a. The identified $Y_2O_3$ nanoparticle with SAED has a cubic crystal structure rotated to the zone axis of [1 0 0]. There is evident micro-porosity between the clustered particles of $Y_2O_3$ on the Cu matrix grain boundary, Fig. 4c. STEM, Fig. 4d, reveals atomic resolution from the $Y_2O_3$ particle with tight and consistent particle-matrix interface without any reaction phase.

The deformation process started the damage by forming cavities in the middle of the specimen, Fig. 5. Most likely damage starts in the triple point and matrix particles interface. The increasing of the load caused grove of cavities by subsequent decohesion of $Y_2O_3$ particles and also widening of cracks on matrix grains boundaries. Since the volume fraction of $Y_2O_3$ particles is small, their distribution does not influence the trajectory of the fracture. We assume that in this case, the grain boundaries play a fundamental role. In the final phase of the fracture, the crack propagates along the grain boundaries.

Decohesion on the matrix-particles interface is a result of different physical properties of phases presented in the system. The Cu matrix has significantly higher thermal expansion coefficient and lower elastic modulus ($\alpha = 17.0 \times 10^{-6}\,\mathrm{K}^{-1}$, $E = 129.8\,\mathrm{GPa}$) than $Y_2O_3$ ($\alpha = 10.0 \times 10^{-6}\,\mathrm{K}^{-1}$, $E = 162\,\mathrm{GPa}$). Large differences in the thermal expansion coefficients result in high-stress gradients, which arise on the interphase boundaries during the hot extrusion. Since $\alpha_{\mathrm{matrix}} > \alpha_{\mathrm{particle}}$, high compressive stresses can be expected. However, because the stress gradients arise due to the temperature changes, during cooling (which increases the stress peaks), their partial relaxation can occur. Superposition of the external load and the internal stresses can initiate cracking at interphase boundaries. This is in accordance also with the dislocation theories which argue that the particles in the composite may cause an increase in the dislocation density as a result of thermal strain mismatch between the ceramic particles and the matrix during preparation and/or thermal treatment. In our case, the coefficient of thermal expansion of the matrix is higher than that of the secondary particles and the resulting thermal tension may relax around the matrix-particle interfaces by emitting dislocations.

According to the initiation and propagation of the cracks observed during the in-situ process of deformation, we tried to propose the model of fracture mechanism, Fig. 6. The three steps of cracks initiation, prop-

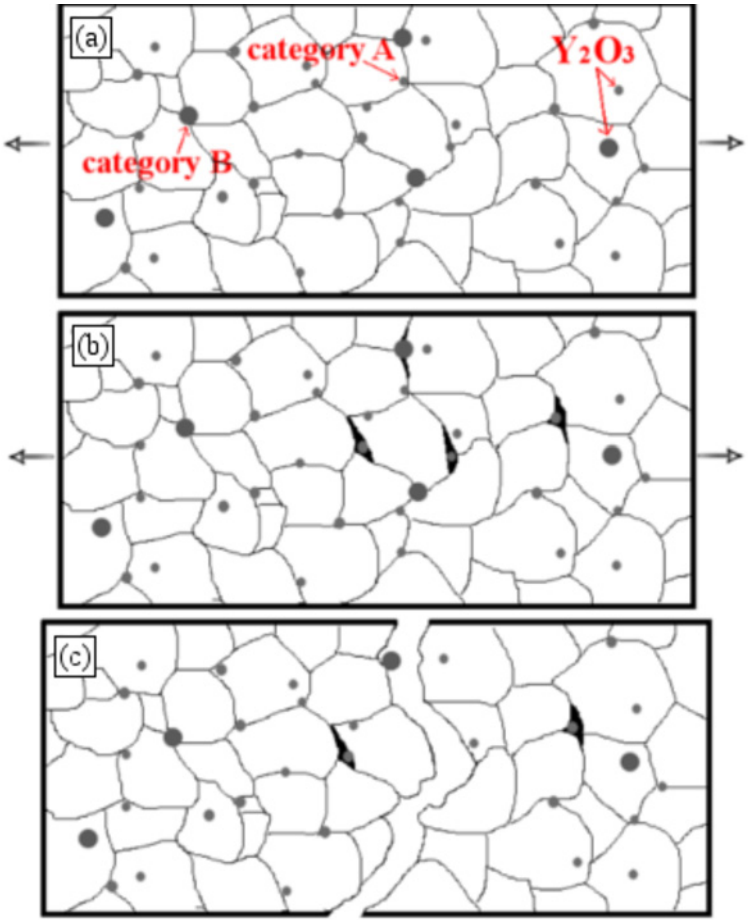


Fig. 6. Model of fracture mechanism of Cu-$Y_2O_3$ composite.

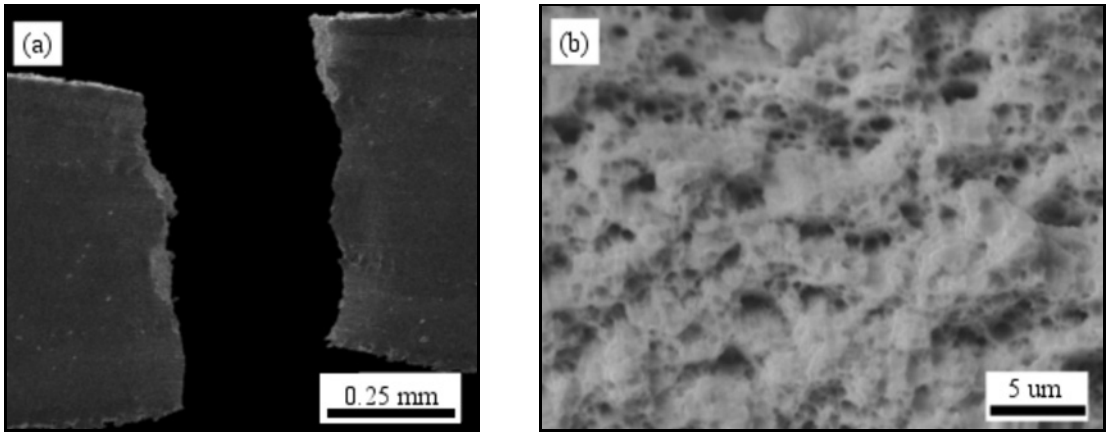


Fig. 7. SEM view of the final fracture, the fracture surface morphology of Cu-$Y_2O_3$ composite.

agation, and coalescence are shown in Fig. 6:

a) the microstructure of the initial state – Cu matrix grains ∼500 nm in diameter, two categories of particles: A – smaller, up to 20 nm and B – larger, 20–100 nm in diameter,

b) increasing of the tensile load caused the formation of the local cracks, Fig. 5, predominantly on the matrix-particles interface,

c) the further increase of the deformation caused propagation and coalescence of the cracks preferentially along with the particle-matrix interface, triple points, grain boundaries and residual micropores.

Figure 7 shows the fracture surface morphology of Cu-$Y_2O_3$ composite and the detail of dimples on the fracture surface. It is evident that fracture surface, Fig. 7, had the transcrystalline ductile character. A

large number of dimples with heterogeneous size distribution are apparent, arising from secondary particles. Still, no particles are evident inside the dimples, which confirms our assumption about the decohesion of particles. The main diameter of dimples was evaluated (approximately 150–200 dimples were measured), the large dimples ($\sim 250$ nm) were created on large particles category B, smaller dimples ($\sim 60$ nm) on the particles category A. According to Gurland-Plateau theory [20], the ductile fracture has three stages: initiation, growth, and coalescence of cavities. Based on the analysis, it can be assumed that cracks were created on the particle-matrix interfaces and in the triple point [21].

## 4. Conclusions

In this work, the structure and its influence on deformation behaviour and fracture mechanism of Cu-$Y_2O_3$ composite were analysed. The analysis of the composite structure showed that the matrix grains have a near-spherical shape with a mean diameter of $\sim 500$ nm, $Y_2O_3$ particles are homogeneously distributed, and the two size categories were determined: A – up to 20 nm and B – 20–100 nm. The "in-situ" tensile test in SEM provides the possibility of direct observation of the deformation processes taking place during loading. Based on the results, the model of the fracture mechanism of Cu-$Y_2O_3$ composite was proposed. The final crack had transcrystalline ductile character.

## Acknowledgement

The work was supported by the Slovak National Grant Agency under the Project VEGA 2/0101/20.

## References

[1] G. Garcés, M. Rodríguez, P. Pérez, P. Adeva, High temperature mechanical properties of Mg-$Y_2O_3$ composite: Competition between texture and reinforcement contributions, Compos. Sci. Technol. 67 (2007) 632–637. doi:10.1016/j.compscitech.2006.07.021

[2] L. Liu, K. Maeda, T. Onda, Z.-C. Chen, Effect of YSZ with different $Y_2O_3$ contents on toughening behavior of $Al_2O_3$/Ba-$\beta$-$Al_2O_3$/$ZrO_2$ composites, Ceramics International 45 (2019) 18037–18043. doi:10.1016/j.ceramint.2019.06.023

[3] Y. Xu, L. Cheng, L. Zhang, X. Luo, W. Zhou, Preparation and mechanical properties of self-reinforced in situ $Si_3N_4$ composite with $La_2O_3$ and $Y_2O_3$ additives, Composites: Part A 30 (1999) 945–950. doi:10.1016/S1359-835X(99)00013-5

[4] Kang Pyo So, Il Ha Lee, Dinh Loc Duong, Tae Hyung Kim, Seong Chu Lim, Kay Hyeok An, Young Hee Lee, Improving the wettability of aluminum on carbon nanotubes, Acta Materialia 59 (2011) 3313–3320. doi:10.1016/j.actamat.2011.01.061

[5] D. Xu, W. J. Lu, Z. F. Yang, J. N. Qin, D. Zhang, In situ technique for synthesizing multiple ceramic particulates reinforced titanium matrix composites (TiB+TiC+$Y_2O_3$)/Ti, J. Alloys and Comp. 400 (2005) 216–221. doi:10.1016/j.jallcom.2005.04.018

[6] K. S. Tun, M. Gupta, Improving mechanical properties of magnesium using nano-yttria reinforcement and microwave assisted powder metallurgy method, Compos. Sci. Technol. 67 (2007) 2657–2664. doi:10.1016/j.compscitech.2007.03.006

[7] A. Genç, S. Coşkun, M. L. Öveçoğlu, Fabrication and properties of mechanically alloyed and Ni activated sintered W matrix composites reinforced with $Y_2O_3$ and $TiB_2$ particles, Materials Characterization 61 (2010) 740–748. doi:10.1016/j.matchar.2010.04.006

[8] N. Selvakumar, S. C. Vettivel, Thermal, electrical and wear behavior of sintered Cu-W nanocomposite, Materials & Design 46 (2013) 16–25. doi:10.1016/j.matdes.2012.09.055

[9] Ang Li, Shuan Ma, Yanjie Yang, Shiqi Zhou, Lan Shi, Mabao Liu, Microstructure and mechanical properties of $Y_2O_3$ reinforced Ti6Al4V composites fabricated by spark plasma sintering, J. Alloys Comp. 768 (2018) 49–56. doi:10.1016/j.jallcom.2018.07.229

[10] G. Carro, A. Muńoz, M. A. Monge, B. Savoini, R. Pareja, C. Ballesteros, P. Adeva, Fabrication and characterization of $Y_2O_3$ dispersion strengthened copper alloys, J. Nuclear Materials 455 (2014) 655–659. doi:10.1016/j.jnucmat.2014.08.050

[11] M. S. Nagorka, C. G. Levi, G. E. Lucas, S. D. Ridder, The potential of rapid solidification in oxide-dispersion-strengthened copper alloy development, Mat. Sci. Eng. A 142 (1991) 277–289. doi:10.1016/0921-5093(91)90666-B

[12] M. Al-Hajri, A. Melendez, R. Woods, T. S. Srivatsan, Influence of heat treatment on tensile response of an oxide dispersion strengthened copper, J. Alloys Comp. 290 (1999) 290–297. doi:10.1016/S0925-8388(99)00227-3

[13] M. A. Atwater, D. Roy, K. A. Darling, B. G. Butler, R. O. Scattergood, C. C. Koch, The thermal stability of nanocrystalline copper cryogenically milled with tungsten, Mater. Sci. Eng. A – Struct. 558 (2012) 226–233. doi:10.1016/j.msea.2012.07.117

[14] Haiou Zhuo, Jiancheng Tang, Nan Ye, A novel approach for strengthening Cu-$Y_2O_3$ composites by in-situ reaction at liquidus temperature, Mater. Sci. Eng. A 584 (2013) 1–6. doi:10.1016/j.msea.2013.07.007

[15] U. Martin, M. Heilmaier, Novel dispersion strengthened metals by mechanical alloying, Adv. Eng. Mater. 6 (2004) 515–520. doi:10.1002/adem.200400410

[16] S. F. Moustafa, Z. Abdel-Hamid, A. M. Abd-Elhay, Copper matrix SiC and $Al_2O_3$ particulate composites by powder metallurgy technique, Mater. Lett. 53 (2002) 244–249. doi:10.1016/S0167-577X(01)00485-2

[17] J. B. Correia, H. A. Davies, C. M. Sellars, Strengthening in rapidly solidified age hardened Cu-Cr and Cu-Cr-Zr alloys, Acta Mater. 45 (1997) 177–190. doi:10.1016/S1359-6454(96)00142-5

[18] M. Khodaei, O. Yaghobizadeh, A. A. Shahraki, S. Es-

maeeli, Investigation of the effect of $Al_2O_3$-$Y_2O_3$-CaO (AYC) additives on sinterability, microstructure and mechanical properties of SiC matrix composites: A review, Int. J. Refr. Met. Hard Mat. 78 (2019) 9–26. doi:10.1016/j.ijrmhm.2018.08.008

[19] Ke Geng, Weijie Lu, Yexia Qin, Di Zhang, In situ preparation of titanium matrix composites reinforced with TiB whiskers and $Y_2O_3$ particles, Mat. Res. Bull. 39 (2004) 873–879. doi:10.1016/j.materresbull.2003.11.008

[20] J. Gurland, J. Plateau, The mechanism of ductile rupture of metals containing inclusions, Trans. ASM 56 (1963) 442–451.

[21] M. Besterci, K. Sulleiová, T. Kvačkaj, Fracture micromechanisms of Cu nanomaterials prepared by ECAP, Kovove Mater. 46 (2008) 309–311.